The effect of surface mechanical attrition treatment on texture evolution and mechanical properties of AZ31 magnesium alloy

Jinhua Peng [a], Zhen Zhang [a,b,*], Peng Guo[a], Zhao Liu[a], Yaozu Li[a], Wei Zhou [c], Yucheng Wu [a,b]

[a] School of Materials Science and Engineering, Hefei University of Technology, Hefei 230009, China

[b] National–Local Joint Research Center of Non-ferrous Metal Materials and Processing Technology, Hefei 230009, China

[c] School of Mechanical and Aerospace Engineering, Nanyang Technological University, 50 Nanyang Avenue, Singapore

Abstract

AZ31 hot-rolled plates with gradient nano-grained surface were produced by surface mechanical attrition treatment (SMAT). The grain size was refined to nanoscale at the surface layer through twinning and dynamic recrystallization (DRX). The micro-hardness of the top layer had a 132% improvement and the increase process could be divided into three stages where the stage at the top surface had the highest increase rate. The (0002) basal texture of basal material was weakened during SMAT which could be reflected by the inclination of (0002) poles, decrease of maximum pole density and divergence of contour lines. The inclined impact direction of steel balls and the sphere balls and non-basal slip at the top surface were responsible for these changes respectively. The yield strength was improved after SMAT and the increment during tensile test was higher than that during compression test due to the different deformation mechanics during tensile and compression test. The weakening of texture had little effect on mechanical properties due to the nano-grains and strong hardening effect at the top surface layer.

Keywords: surface mechanical attrition treatment; macro-texture; finite element simulation; mechanical properties

The effect of surface mechanical attrition treatment on texture evolution and mechanical properties of AZ31 magnesium alloy

Abstract

AZ31 hot-rolled plates with gradient nano-grained surface were produced by surface mechanical attrition treatment (SMAT). The grain size was refined to nanoscale at the surface layer through twinning and dynamic recrystallization (DRX). The micro-hardness of the top layer had a 132% improvement and the increase process could be divided into three stages where the stage at the top surface had the highest increase rate. The (0002) basal texture of basal material was weakened during SMAT which could be reflected by the inclination of (0002) poles, decrease of maximum pole density and divergence of contour lines. The inclined impact direction of steel balls and the sphere balls and non-basal slip at the top surface were responsible for these changes respectively. The yield strength was improved after SMAT and the increment during tensile test was higher than that during compression test due to the different deformation mechanics during tensile and compression test. The weakening of texture had little effect on mechanical properties due to the nano-grains and strong hardening effect at the top surface layer.

Keywords: surface mechanical attrition treatment; macro-texture; finite element simulation; mechanical properties

1. Introduction

Magnesium (Mg) alloys have gained increasing interest in the aerospace and automotive industries due to their significant weight reduction [1]. However, the deficiency of slip systems and strong anisotropy of magnesium alloys resulted in poor ductility and workability at room temperature, which was the main reason of their limited application [2,3]. Hence, the ductility should be enhanced in order to be used for structural components. Many methods have been conducted on magnesium alloys to improve their deformability, such as grain refinement and texture weakening [4-7].

Texture weakening was an effective way to improve the ductility, such as equal channel angular extrusion (ECAE) [8] and friction stir process (FSP) [9], however the yield strength decreased significantly [10-12] due to the activation of abundant basal slip and {10-12} twinning. Grain refinement could improve the strength and ductility simultaneously but the increment was finite [13]. Thus it was necessary to explore a more effective way to improve the comprehensive mechanical properties of Mg alloys. As reported, a coarse-grained copper substrate with a nano-grained copper film was obtained by surface mechanical grinding treatment (SMGT) [14], the yield strength was twice that of the coarse-grain sample as well as higher elongation. This would be also an effective way to improve the mechanical properties for Mg alloys.

In recent years, surface mechanical attrition treatment (SMAT) was conducted to generate a gradient nano-grained film at the surface of Mg alloys as SMGT [15,16]. The grain size could be refined to 30±5nm through twinning and dynamic recrystallization (DRX) [17]. Grain refinement and dislocation accumulation at the surface layer led to a significant increment in micro-hardness [17,18]. The mechanical properties, especially for yield strength, also had a significant improvement [19]. However, as an important influencing factor [20,21], the texture evolution during SMAT was

rarely studied and the effect of texture on mechanical properties was still unclear.

In this study, SMAT was conducted on AZ31 hot-rolled plates to generate nano-grained film. The micro-structure was observed by optical microscopy (OM) and transmission electron microscopy (TEM). The micro-hardness distribution was studied combined with the microstructure at different layer. Moreover, the texture evolution during SMAT was analyzed by X-Ray diffraction (XRD) and the finite element (FE) simulation was used to analyze the reasons for texture variation. The effect of SMAT on tensile and compression properties were studied by tensile and compression tests along RD.

2. Materials and methods

The material used in current study was hot-rolled commercial AZ31 magnesium alloy plates, with thickness of 2.2mm and 5mm. The nominal composition is 3% Al, 1% Zn and the balance Mg. Round samples with a diameter of 49mm were cut from 5mm thick plate, and put into SMAT processing using SPEX8000M high energy ball milling machine. The sample was installed on the top side of the pot. The processing time was 30min, 60min and 90min respectively for both side. In order to study the effect of the impacting style of steel balls and for the tensile test, two kinds of samples (sample A and sample B) were machined from 2.2mm hot-rolled plate, and the processing time of each side was 60min. The difference was that sample A was installed on the top side of the pot while sample B was put inside the pot.

Microstructure observation was carried out by optical microscopy (OM) and transmission electron microscopy (TEM). The microstructure on RD-TD plane in different depth was examined layer by layer by grinding off the top side gradually. Φ3*0.1mm discs was adopted as TEM sample with a plain end at the processed surface and then the sample was fabricated by focused ion beam (FIB). Macro-texture was measured on the treated plane for SMATed samples and RD-TD plane for rolling plates, with Panalytical X-ray diffractometer in Schulz reflection geometry, all of these samples were cleaned by the solution of nitric acid and alcohol and tested with same parameters. The micro-hardness on side plane and treating plane was tested with 300g load for 10s. Tensile and compression test were tested along RD with a strain rate of 0.001/s at room temperature. The tensile samples had a gage length of 18mm and width of 4mm while the compression samples had a dimensions of 2mm*3mm*T (thickness of samples). On the other hand, the impacting process of steel balls from different direction were simulated by Deform software and the strain and material flow were extracted for analyzing.

3. Results and discussion

3.1 Microstructure observation. Fig. 1a gives the schematic illustration of the SMAT process. The sample with diameter of 49mm and thickness of 5mm was installed on the top side of the pot. Meanwhile steel balls with diameter of 8mm were put into the pot. In order to enhance the impact energy, the pot conducts a motion with a path of three-dimensional 8-font during the SMAT process which was shown in Fig. 1b. Compared with the traditional way where the pot vibrate up and down, the impact direction of steel balls in this paper would be regular due to the special motion trail of the pot. Most of steel balls would impact the sample with an angle and resulted in an asymmetric strain. Figure.1c shows the macrostructure of sample after 60min SMAT. Obviously, the round black region on RD-TD plane in Fig. 1c-B was SMATed zone where oxidization took place during SMAT. At the side view on ND-TD plane, it was evident that the sample had underwent serve

plastic deformation and the SMATed zone had curved in due to the impacting of the steel balls. Two different zone appeared after polishing and etching, the surface layer was white while the interior zone was dark, the microstructure of these two regions were shown in Fig. 2.

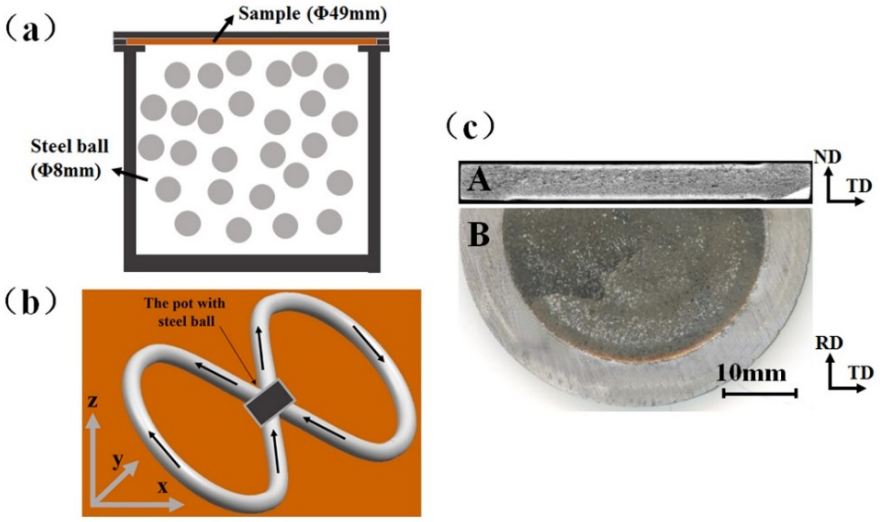

Fig. 1. Schematic illustration of (a) SMAT technique, (b) motiving trail of the pot, and (c) the macro-structure on ND-TD plane and RD-TD plane of SMATed sample

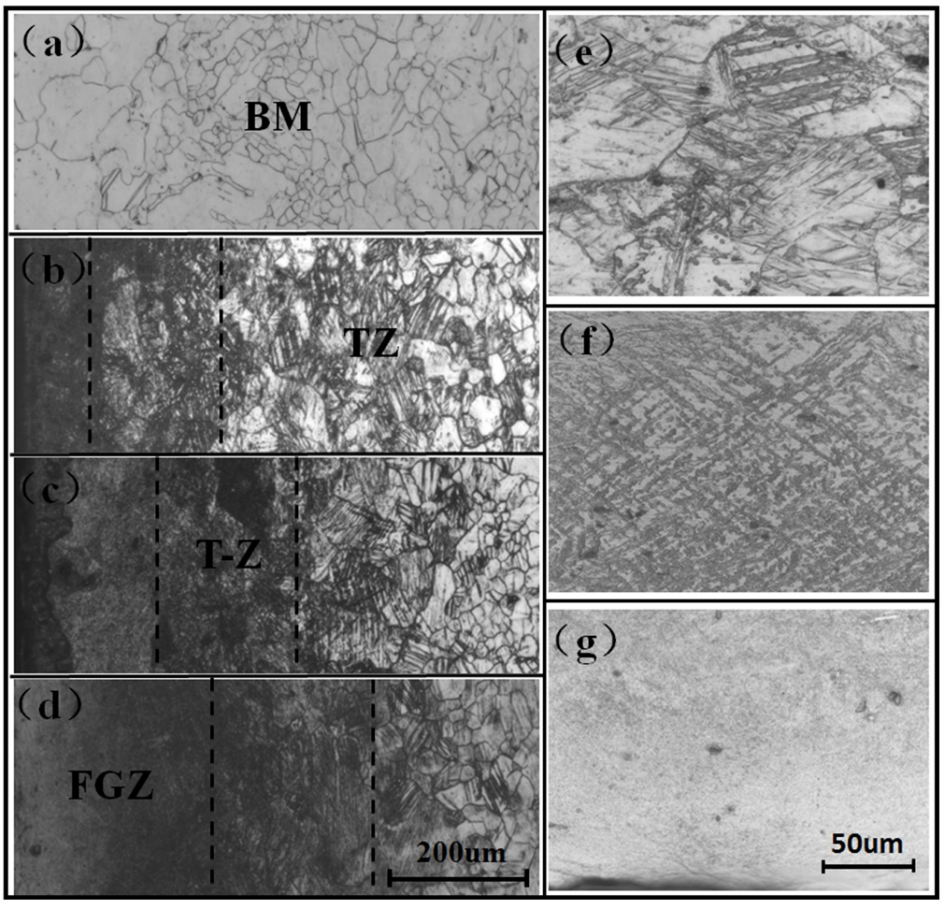

Fig. 2. The microstructure of (a) dark region (base material (BM)) and white regions for (b) 30min, (c) 60min and (d) 90min SMATed samples, and different regions of the surface layer: (e) twinning zone (TZ), (f) transition zone (T-Z) and (g) fine grain zone (FGZ).

Fig. 2a shows the microstructure of dark region, it could be clearly seen that the dark region showed coarse grains with an average grain size of 50um which was consistent with the base material. It mean that the interior zone underwent little change during SMAT. The microstructure of surface layer was shown in Fig. 2b-d, the processing time was 30min, 60min and 90min respectively. Clearly, a gradient structure came into being at the surface layer and it could be mainly divided into three different regions-twinning zone (TZ), transition zone (T-Z) and fine grain zone (FGZ) depending on the different microstructure. The typical microstructures of these zones were shown in Fig.2e-g. Plenty of twins could be found during TZ, the twin types and distribution was intricate due to the complicated stress state during SMAT and slight recrystallized grains could be found at the edge of twins. Closing to the surface, the number of recrystallized grains increased significantly and located on a series of parallel lines during T-Z. The FGZ was formed when the recrystallized grains fill the whole grains and the grain was too small to be distinguished by optical microscope, so TEM was applied on the microstructure observation in FGZ.

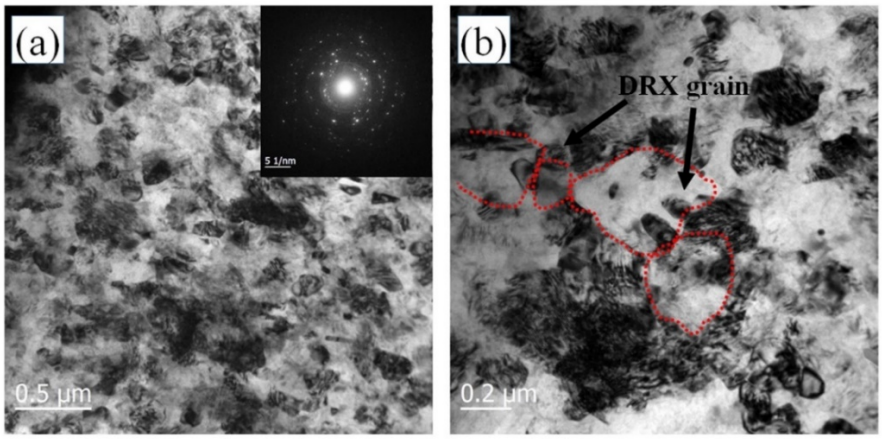

Fig. 3. Bright filed TEM images showing (a) the microstructure of FGZ with the corresponding SAED patterns at the top right corner and (b) the DRX grains along the grain boundary of the 60min SMATed sample.

Fig. 3 shows the TEM examination of the surface layer about 80um from the surface of the sample after 60min treatment. Clearly, a nanostructured surface layer was developed. The average grain size was about 200nm which was significantly refined comparing with the base material. Meanwhile abundant defects were found in this area and the dynamic recrystallization (DRX) was in progress, some DRX grains were forming at the side of the grain boundaries, as shown in Fig. 3b. In order to further reveal the process of the formation of the nano-grains, the microstructure of different layers on RD-TD plane were received by grinding the upper surface gradually, as shown in Fig.4. The formation process of the nano-grains would be clear through analyzing these pictures. Tensile twinning (Fig.4e) would dominated the deformation in the initial stage where the strain (resulting from the impact of the steel balls) was small. With further straining, tensile twinning grew up and disappeared gradually, a great deal of paralleled contract twins (Fig.4d) formed in the grains. As a strong pinning point, plenty of dislocation would pile up at the contract twin boundary. With the increased strain, the high stored energy promoted the occurrence of DRX along the contract twins. Therefore, it could be seen in Fig.4bcd that most of the DRX grains distributed along some paralleled lines and fill the whole grains finally (Fig.4b). DRX would keep on when the grain was full of DRX grains, the DRX grains would be refined again by SMAT and the nano-grain was

obtained on the surface finally. All in all, twinning and DRX played important roles during the formation of nano-grains and dominated the whole process.

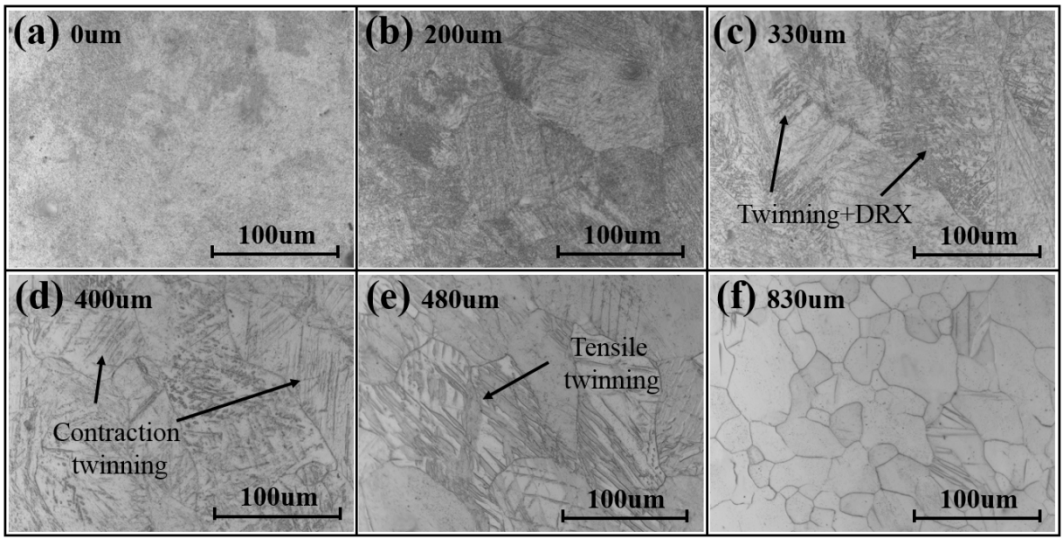

Fig. 4. The microstructure on RD-TD plane with different depth and the depth of each picture was marked on the top left corner

3.2 Micro-hardness distribution on side plane and treated plane. In order to investigate the influence of SMAT on mechanical properties of the experimental material, the micro-hardness distribution on ND-TD plane were measured, as shown in Fig. 5a. Clearly, the micro-hardness of the base material distributed uniformly along depth, which was about 50HV. After SMAT, the micro-hardness of the top surface layer increased significantly the maximum value was 108HV for 90min SMATed sample, with a 116% increment. With the increase of depth from surface, the micro-hardness decreased rapidly and the lowest value in the middle of the sample was almost equal to that of base material. On the other hand, the micro-hardness increased gradually with SMAT duration from 30min to 90min, but the increment was lower and lower due to the limitation of grain refinement through SMAT.

As shown in Fig.4, the microstructure of different layers changes gradually. Following the microstructure observation, the micro-hardness of different layers on RD-TD plane was also tested to reveal the relationship between the microstructure and micro-hardness, as shown in Fig.5b. Meanwhile, the typical microstructure in Fig.4 was marked in Fig.5b where the microstructure and the micro-hardness were in the same layer. It clearly shows that the micro-hardness decreased gradually with the increased distance from the top surface, as the distribution on ND-TD plane. It should be noted that the highest value on RD-TD plane was higher than that on ND-TD plane which had a 132% improvement. The reason was that the micro-hardness of the top surface was impossible to test on RD-TD plane, the highest micro-hardness on RD-TD plane was tested on the subsurface. Combing with the microstructure of different layers (Fig.4), the micro-hardness increment could be divided into three stages. At the first stage, the grains underwent nearly no strain during SMAT and kept coarse grains as the base material, so the micro-hardness of these zone remained unchanged and the increment rate of micro-hardness was 0 (K3=0). Closing to the surface, the micro-hardness started to increase with a slow rate (K2), the grain refinement induced by twinning (primarily tensile twinning) would be responsible for the increment in this stage. The contract twinning came into being when the strain increased, abundant dislocation piled up and DRX grain appeared along with

contract twins, these changes led to grain refinement and strain hardening quickly. So the micro-hardness increased with higher rate (K1). The special gradient structure and deformation mechanics of Mg alloy led to different stages of micro-hardness increment and the increment rate decreased with the increased distance from upper surface.

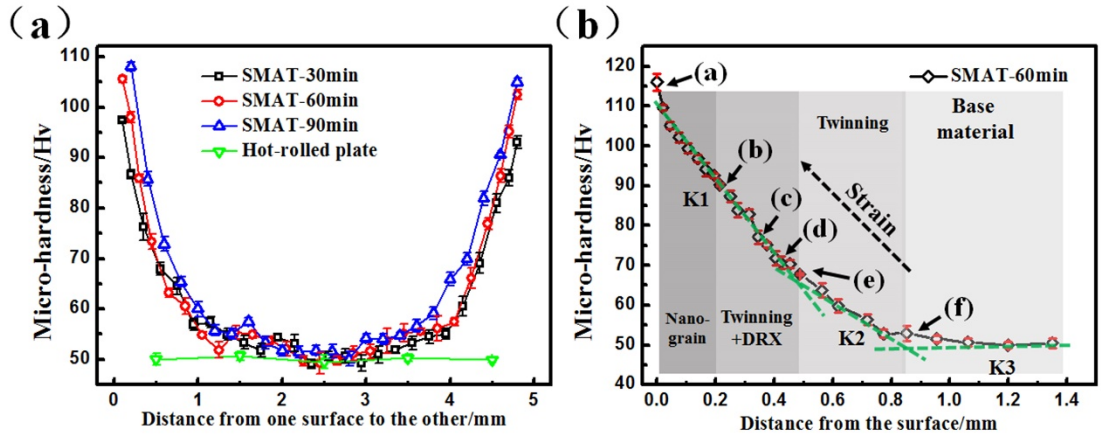

Fig. 5. The micro-hardness distribution along depth on (a) ND-TD plane and (b) RD-TD plane before and after SMAT. The corresponding microstructure of different layer from Fig.4 was marked in (b).

3.3 Texture variation during SMAT. As reported [22,23], (0002) basal texture often formed when Mg alloys underwent plastic deformation due to the hexagonal close-packed (HCP) structure. The basal texture had a significant effect on the mechanical properties of Mg alloys [24]. Thus it was important to reveal the texture variation during SMAT. Firstly, XRD measurement was conducted on samples before and after SMAT and the results were shown in Fig. 6a. Compared with the base material, the diffraction lines broadened and the diffraction intensity of (0002) plane decreased significantly after SMAT which could be mainly on account of grain refinement, lattice distortion as well as texture weakening. In order to distinguish these reasons, the 90min SMATed sample was annealed at 300℃ to remove the effect of lattice distortion and grain refinement, the results was shown in Fig. 6b. Clearly, the intensity of (0002) plane increased after annealing due to the recrystallization, but it was still lower than that of the base material. After annealing, the only factor of the decreased intensity was texture weaken indicating that the (0002) basal texture was weakened during SMAT. However the specific distribution of texture was still unclear, so the macro-texture was tested by XRD to reveal texture variation during SMAT.

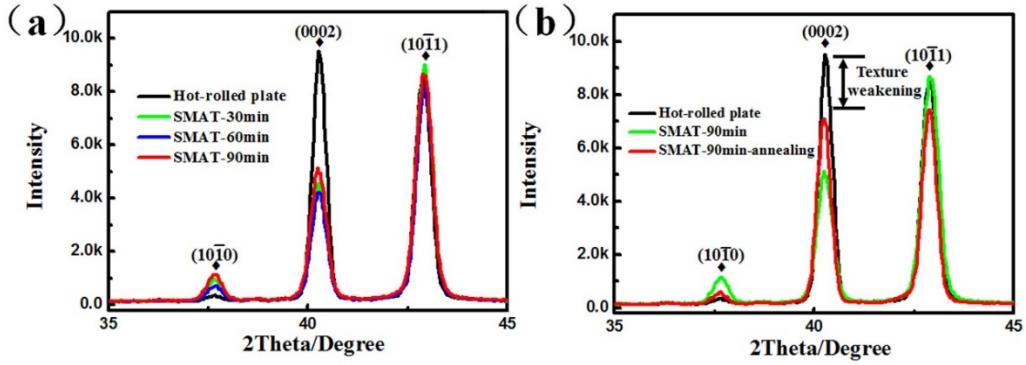

Fig. 6. XRD patterns of (a) the hot-rolled plate and SMATed samples and (b) the 90min SMATed sample before and after annealing.

The (0002) pole figures of samples before and after SMAT were shown in Fig. 7a-d. It could be clearly seen that the starting material showed a typical strong (0002) basal texture where the <0001> orientation was aligned with ND. After SMAT, the basal texture was weakened assuredly which could be reflected through three categories and some trend could be seen with SMAT duration. Firstly, the (0002) poles inclined from ND to RD-TD plane and the inclined angle increased gradually from 30min to 90min SMAT. The inclined angle was measured through (0002) poles and plotted in Fig. 7e. Clearly, the inclined angle of base material was only 3°and it increased quickly with the prolonged treating time, about 41°for 90min SMATed sample. Secondly, the maximum pole density decreased gradually during SMAT (Fig.7e) and the maximum pole density of 90min sample was only 15481, 25% of the base material. Thirdly, the contour lines during pole figures were diverging. The intensity distribution along the line between the center of pole figure and the maximum pole density point were plotted in Fig.7f. It was clear that the base material had a sharp peak and the peak became widen with SMAT duration.

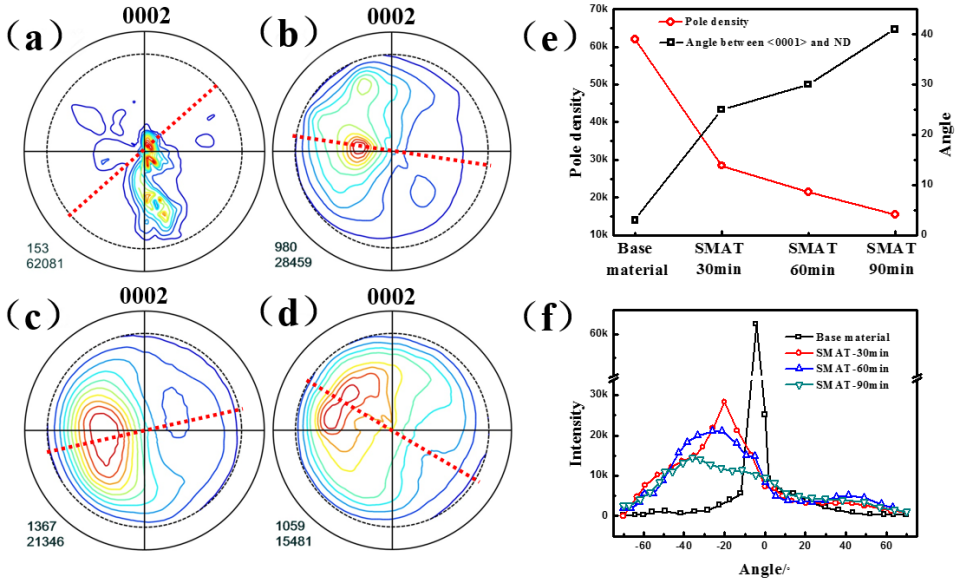

Fig. 7. (0002) poles of (a) hot-rolled plate and SMATed samples: (b) 30min, (c) 60min, (d) 90min and (e) the maximum pole density distribution and the angle between <0001> poles and ND and (f) the intensity distribution along the lines between the center of pole figure and the maximum pole density point for samples before and after SMAT.

As mentioned above, crystallographic texture was often easily formed in Mg alloys when it underwent plastic deformation. During SMAT, the plastic deformation was induced by the impacting of the steel balls, so the transformation of texture would be resulted from the impacting of steel balls. In view of the motion trail of the pot (Fig. 1b), the majority of steel balls would impact the sample with an angle which would be the reason of the inclined (0002) poles. In order to investigate the effect of the motion trail of steel balls on texture variation, SMAT was conducted on two same samples from 2.2mm hot-rolled plate, sample A and sample B, simultaneously. Sample A was installed on the top side of the pot while sample B was put in the pot. Steel balls would impact sample A aslant as stated above while the steel balls would impact sample B vertically because sample B in the pot had a similar motion trail with steel balls.

3.4 Reasons for texture weakening. Fig. 8. shows the macro-texture of the 2.2mm hot-rolled plate and sample A, B. It was clearly seen that, for sample A and B, the maximum pole density

decreased observably and the contour lines were diverging as the results shown in Fig. The only difference was that the (0002) pole of sample A inclined from ND to RD-TD plane while the (0002) pole of sample B had almost no inclination. It indicated that the motion trail of steel balls was reasonable for the inclination of (0002) basal texture. The decrease of maximum pole density and the divergence of contour lines would be resulted from other factors. In order to make further investigation of the reasons for inclination of (0002) basal texture, the decrease of maximum pole density and the divergence of contour lines, the impacting process of steel balls from different direction during SMAT was simulated by Deform software.

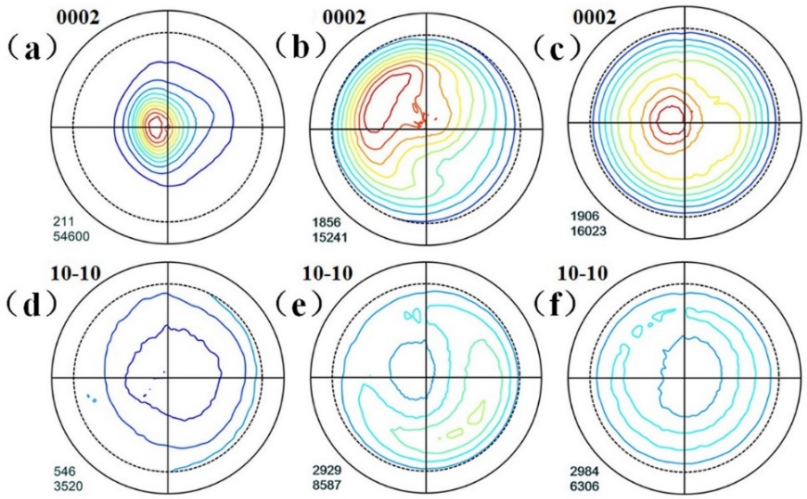

Fig. 8. (0002) poles and (10-10) poles of (a), (d) hot-rolled plate and 60min SMATed samples: (b), (e) sample A and (c), (f) sample B.

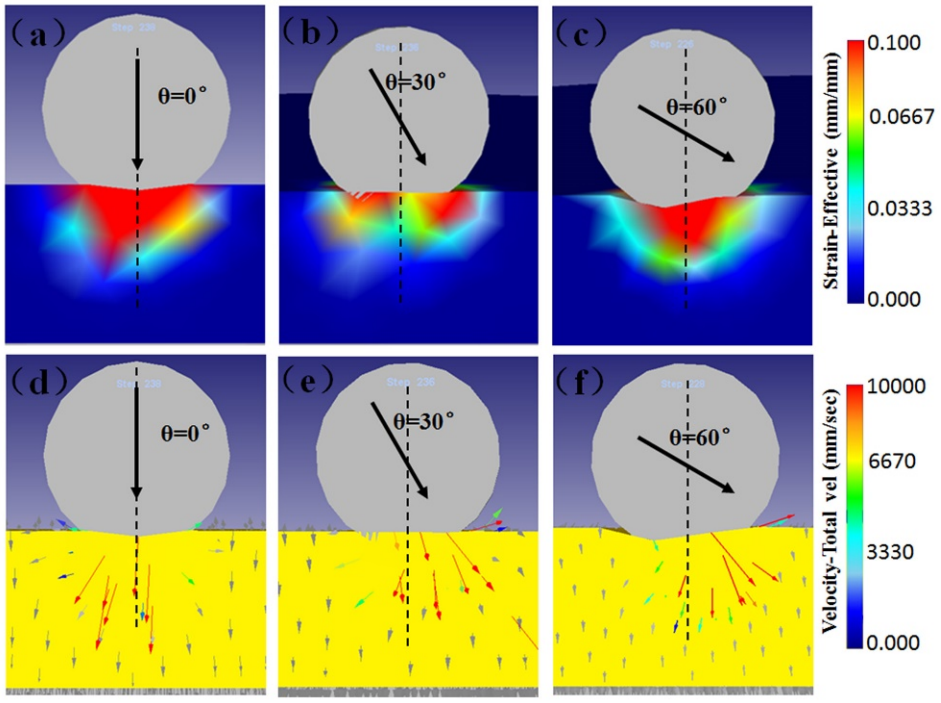

Fig. 9. The strain and material flow during the impact process with steel balls from different direction with an angle of (a), (d) 0°, (b), (e) 30°and (c), (f) 60° between ND and impact direction.

Fig. 9 shows the strain distribution and material flow when steel balls impact the sample from different direction. Clearly, the strain distribution and material flow were different for different impact direction. When steel ball impacted the sample along ND, the strain was distributed under the ball with an ellipsoidal shape and the main direction of material flow was almost paralleled with the impacting direction. And when the direction of steel ball fell away from ND with an angle of 30 or 60 degrees, the strain inclined to one side and the main material flow direction also fell away from ND though the material flow was somewhat scattered. Precisely, the strain and material flow was induced by the force from steel balls and in consideration of the different state of sample A and B. The stress state of sample A and B could be simplified as Fig.10a and b, respectively, where ball A impacted sample with an angle θ and ball B impacted sample along ND. Different impact direction resulted in different stress state and then caused different condition of strain and material flow.

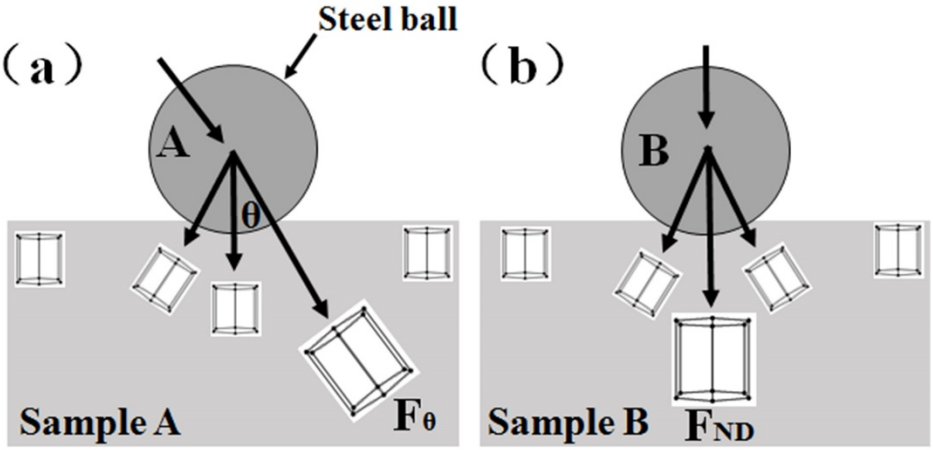

Fig.10. Schematic illustration of the steel ball from different direction: (a) inclining and (b) paralleling with ND.

Under the loading force, slip and twinning would be activated to coordinate plastic deformation. However, during the later period of SMAT, basal slip would be the dominated deformation mechanism because twinning was suppressed due to refined grains [25,26]. And abundant basal slip would result in grain rotation if the slip plane were either parallel or perpendicular to the direction of applied stress [27,28]. So when steel ball A impacted sample A with an angle θ, both the plane of slip and the direction of slip tend to rotate vertically to the axis of compression which could be the impact direction. As a result, the repeated multidirectional impact of steel balls resulted in the inclination of (0002) basal texture for sample A. But for sample B, the main force was perpendicular to the slip plane ((0002) plane). So there would be none grain rotation and texture inclination. In a word, the inclination of (0002) basal texture was resulted from the different impact direction of steel balls.

On the other hand, strictly speaking, the contact surface between steel balls and samples was not a plane, but a camber concave. Hence, the stress and material flow induced by steel balls would be somewhat scattered as shown in Fig. 9 and Fig.10 and the scattered force also led to slight grain rotation. Whether steel balls impacted the sample along ND or with an angle, some grains would rotate to an orientation where the (0002) plane paralleling with the spherical surface as shown in Fig.10. These rotated grains resulted in the reduction of maximum pole intensity and diffusion of basal texture. And the maximum pole intensity would decreased gradually and the contour lines were more diverging with SMAT duration.

In addition, in consideration of the grain size of the surface layer and the huge impact force, non-basal slip systems [29,30], including prismatic slip and pyramidal slip, could be activated which also would lead to some grain rotation. The rotated grains also led to the decrease of maximum pole intensity and the divergence of contour lines. All in all, the impact direction of steel balls were responsible for the inclination of basal texture while the sphere balls and non-basal slip were responsible for the significant decrease of maximum pole intensity and the divergence of contour lines.

3.5 Mechanical properties from uniaxial tensile and compression tests. A gradient nano-grain layer was formed at the surface of samples during SMAT which would improve the strength of base material. However, it is contrary that texture weakening could decrease the strength significantly. Therefore, in order to reveal the effect of SMAT on mechanical properties, uniaxial tensile and compression tests along RD were conducted on sample A, B and 2.2mm hot-rolled plate. The engineering stress vs. strain curves were shown in Fig. 11a and b.

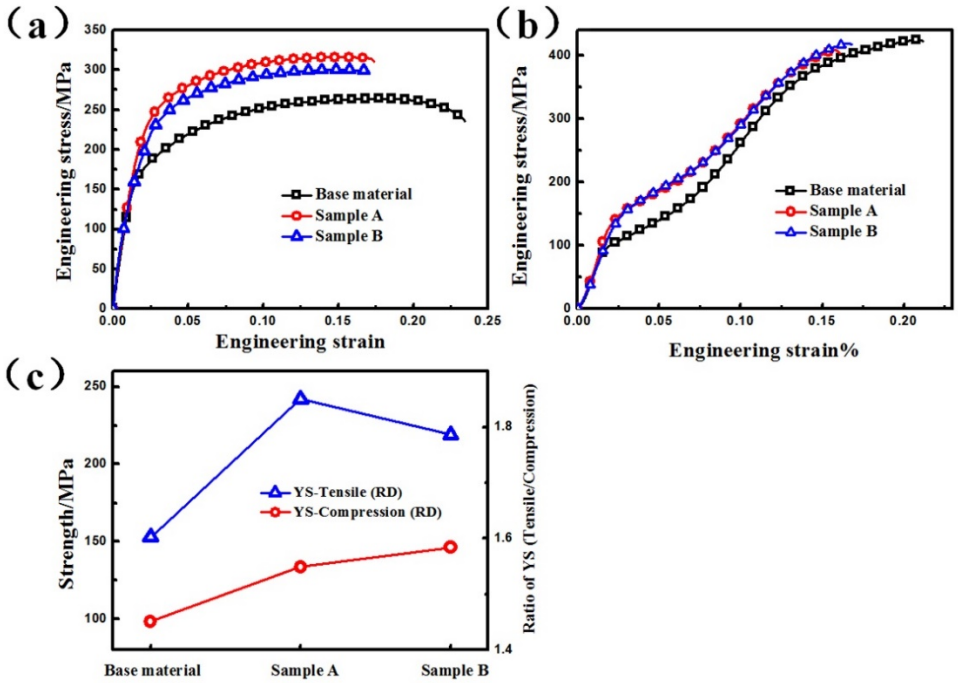

Fig. 11. The engineering stress vs. strain curves during (a) tensile and (b) compression test of samples before and after SMAT; (c) the yield strength (YS) distribution during tensile and compression test.

It was clearly seen that the yield strength and ultimate tensile strength during tensile test were improved significantly after SMAT. However the elongation decreased which was consistent with pervious works [19]. The grain refinement and the accumulation of dislocation during the surface made contribution to the improvement of strength. During compression test, the yield also increased while the compression strength and elongation decreased slightly after SMAT. It should be noted that the increment of yield strength during tensile test was visibly higher than that during compression test as shown in Fig.11c. During tensile test, dislocation slip was the main deformation mechanics. The slip resistance would increase quickly when abundant defects forming during SMAT which made the yield strength increase significantly. But during compression test, {10-12} twinning was the dominated deformation mechanics. The hardening of the surface layer had little

effect on the activation of {10-12} twinning during base material, so the increment of yield strength during compression test was lower than that in tensile test.

As reported, the yield strength would decrease significantly when the basal texture was weakened by FSP or ECAP in spite of the refined grains due to the reduced CRSS of basal slip and activation of {10-12} twinning [6,12]. However, the yield strength increased obviously whether in tensile or compression test though the texture was weakened during SMAT. Especially for sample A which had an inclined basal texture, the yield strength was the highest during tensile test and the compression curve was almost coincident with that of sample B. The results indicated that the texture softening effect was removed during SMAT and there would be two reasons for this. Firstly, the grain size of the surface layer was refined to nanoscale, twinning was suppressed and more slip systems were activated [29]. Consequently the texture softening effect which resulted from the activation of twinning and basal slip was weak. Secondly, base material underwent strong hardening during SMAT and there were plenty of dislocation during the surface layer which could improve the strength effectively. The texture softening effect would be covered up by the hardening effect. As a result, the texture weakening during SMAT had little effect on the mechanical properties.

4. Conclusions

In summary, a gradient nano-grained layer was received by SMAT on the hot-rolled AZ31 magnesium alloys. The grain size was refined to 200nm due to the severe plastic deformation and dynamic recrystallization. Grain refinement and dislocation accumulation resulted in a significant micro-hardness improvement at the surface layer. The increment of micro-hardness could be divided into three stages depending on the microstructure at different layers. The stage at the top surface had the highest increase rate due to the frequent grain refinement and dislocation multiplication.

The basal texture was weakened during SMAT including the inclination of (0002) poles, the decrease of maximum pole density and the divergence of contour lines. The inclined impact direction of steel balls was responsible for the inclination of (0002) poles while the sphere balls and non-basal slip at the top surface were responsible for the significant decrease of maximum pole intensity and the divergence of contour lines. The yield strength was improved during tensile and compression test due to grain refinement and accumulation of dislocation and the increment of yield strength during tensile test was higher than that in compression test. The texture weakening had little effect on mechanical properties due to the nano-grains and strong hardening effect at the surface layer.

References

[1] B.L. Mordike, T. Ebert, Magnesium: Properties-applications-potential, Mater. Sci. Eng. A 302 (2001) 37-45.

[2] S.R Agnew, J.W. Senn, J.A. Horton, Mg sheet metal forming: Lessons learned from deep drawing Li and Y solid-solution alloys, Metals Mater. Soc. (TMS) 58 (2006) 62-69.

[3] ASM speciality handbook, Magnesium and magnesium alloys, Materials Park (OH): ASM international, 1999.

[4] S. Biswas, H.G. Brokmeier, J.J. Fundenberger, S.Suwas, Role of deformation temperature on the evolution and heterogeneity of texture during equal channel angular pressing of magnesium, Mater. Charact. 102 (2015) 98-102.

[5] S.M. Razavi, D.C. Foley et al, Effect of grain size on prismatic slip in Mg–3Al–1Zn alloy, Scr. Mater. 67 (2012) 439-442.

[6] Q. Miao, L.X. Hu, H.F. Sun & E.D. Wang, Grain refining and property improvement of AZ31 mg alloy by hot rolling, Tran. Nonferr. Metal. Soc. 19 (2009) 326-330.

[7] R.K. Mishra, A.K. Gupta, P.R. Rao et al, Luo. Influence of Cerium on Texture and Ductility of Magnesium Extrusions, Scr. Mater. 59 (2008) 562-565.
[8] K.R. Gopi, & H.S. Nayaka, Microstructure and mechanical properties of magnesium alloy processed by equal channel angular pressing (ECAP), Mater. Today Proc. 4 (2017) 10288-10292.
[9] W. Woo, H. Choo, D.W. Brown et al, Texture variation and its influence on the tensile behavior of a friction-stir processed magnesium alloy, Scr. Mater. 54 (2006) 1859-1864.
[10] W.J. Kim, Y.K. Sa, Micro-extrusion of ECAP processed magnesium alloy for production of high strength magnesium micro-gears, Scr. Mater. 54 (2006) 1391-1395.
[11] W. Yuan, S.K. Panigrahi, J.Q. Su et al, Influence of grain size and texture on Hall–Petch relationship for a magnesium alloy, Scr. Mater. 65 (2011) 994-997.
[12] T. Mukai, M. Yamanoi, H. Watanabe et al, Ductility enhancement in AZ31 magnesium alloy by controlling its grain structure, Scr. Mater. 45 (2001) 89-94.
[13] A. Yamashita, Z. Horita & T.G. Langdon, Improving the mechanical properties of magnesium and a magnesium alloy through severe plastic deformation, Mater. Sci. Eng. A 300 (2001) 142-147.
[14] T.H. Fang, W.L. Li, N.R. Tao, K. Lu, Revealing extraordinary intrinsic tensile plasticity initialization in gradient nano-grained coopper, Science. 331 (2011) 1587-1590.
[15] L. Zhang, Y. Zou, H. Wang et al, Surface nanocrystallization of Mg-3 wt.% Li-6 wt.% Al alloy by surface mechanical attrition treatment, Mater. Charact. 120 (2016) 124-128.
[16] Y.H. Wei, B.S. Liu, L.F. Hou et al, Characterization and properties of nanocrystalline surface layer in Mg alloy induced by surface mechanical attrition treatment, J. Alloys Compd. 452(2) (2008) 336-342.
[17] H.Q. Sun, Y.N. Shi, M.X. Zhang et al, Plastic strain-induced grain refinement in the nanometer scale in a Mg alloy, Acta Mater. 55(3) (2007) 975-982.
[18] X. Liu, Y. Liu, B. Jin et al, Microstructure Evolution and Mechanical Properties of a SMATed Mg Alloy under In Situ SEM Tensile Testing, J. Mater. Sci. Technol. (3) (2016) 224-230.
[19] X. Meng, M. Duan, L. Luo et al, The deformation behavior of AZ31 Mg alloy with surface mechanical attrition treatment, Mater. Sci. Eng. A 707 (2017) 636-646.
[20] Y. Wang, H. Choo, Influence of texture on Hall–Petch relationships in an Mg alloy, Acta Mater. 81 (2014) 83-97.
[21] Y.N. Wang, C.L. Chang, C.J. Lee et al, Texture and weak grain size dependence in friction stir processed Mg–Al–Zn alloy, Scr. Mater. 55(7) (2006) 637-640.
[22] J. Hiscocks, B.J. Diak, A.P. Gerlich, M.R. Daymond, Formation mechanisms of periodic longitudinal microstructure and texture patterns in friction stir welded magnesium AZ80, Mater. Charact. 122 (2016) 22-29.
[23] J.A.D. Valle, F. Carreño & O.A. Ruano, Influence of texture and grain size on work hardening and ductility in magnesium-based alloys processed by ECAP and rolling, Acta Mater. 54 (2006) 4247-4259.
[24] H. Yu, C. Li, Y. Xin et al, The mechanism for the high dependence of the Hall-Petch slope for twinning/slip on texture in Mg alloys, Acta Mater. 128 (2017) 313-326.
[25] M.R. Barnett, A rationale for the strong dependence of mechanical twinning on grain size, Scr. Mater. 59 (2008) 696-698.
[26] L.H. Zhang, Y. Zou et al, Surface nanocrystallization of Mg-3 wt.% Li-6 wt.% Al alloy by surface mechanical attrition treatment, Mater. Charact. 120 (2016) 124-128.
[27] Sidny H. Avner, Introduction to physical metallurgy, second edition, New York, 1974.
[28] B.D. Cullity, S.R. Srock. Elements of X-Ray Diffraction. Addison-Wesley publishing company. 1956.
[29] J. Koike, T. Kobayashi, T. Mukai T, et al, The activity of non-basal slip systems and dynamic recovery at room temperature in fine-grained AZ31B magnesium alloys, Acta Mater. 51 (2003) 2055-2065.

[30] L. Sun, J. Bai, F et al, Exceptional texture evolution induced by multi-pass cold drawing of magnesium alloy, Mater. Des. 135 (2017) 267-274.